PSBarrier vs. Conduit Behavior of Faults Near Salt: Examples from the Gypsum Valley Salt Wall*

Lillian Lueck[1] and Mark Fischer[1]

Search and Discovery Article #42451 (2019)**
Posted September 23, 2019

*Adapted from poster presentation given at AAPG 2019 Annual Convention & Exhibition, San Antonio, Texas, May 19-22, 2019

DOI:10.1306/42451Lueck2019

[1] Northern Illinois University, DeKalb, IL, United States (lirueck@gmail.com; mfischer@niu.edu)

Abstract

Rising salt bodies create unique deformation patterns and faulting associated with salt tectonics. These fracture networks can influence the hydrological behavior of rocks near salt bodies by acting as barriers or conduits for the movement of fluids like sedimentary brine, meteoric water, hydrocarbons and various ore-forming fluids. Studying the field characteristics of brittle deformation near salt can help identify and rank the significance of variables associated with the compartmentalization of subsurface fluids by faults adjacent to salt. In the southwestern portion of the Paradox Basin, in southwestern Colorado, the southern end of the Gypsum Valley salt wall features a NW-trending counter-regional fault and two SW-trending radial faults. We combined field and laboratory analyses to investigate the paleohydrological behavior of these faults. Field observations suggest radial fractures formed first and are enhanced by the two radial faults, while concentric fractures formed later. Fracture intensity generally decreases with distance from the radial faults suggesting that some fractures were induced by faulting. Microtextures in calcite veins suggest mineralization was primarily post-kinematic. Stable isotopes of carbon and oxygen in calcite show the presence of two paleofluid types: meteoric water or sedimentary brines. Both are found along the radial faults, while one type is found along the counter-regional fault suggesting the faults in this area served as conduits to flow, but that different fluids may have moved along each type of fault. There is no partitioning of paleofluid types across the faults, indicating that they did not compartmentalize the regional, kilometer-scale fluid system.

References Cited

Bons, P.D., M.A. Elburg, and E. Gomez-Rivas, 2012, A Review of the Formation of Tectonic Veins and Their Microstructures: Journal of Structural Geology, v. 43, p. 33-62.

Escosa, F.O., M.G. Rowan, K.A. Giles, K.T. Deatrick, A.M. Mast, R.P. Langford, T.E. Hearon IV, and E. Roca, 2018, Lateral Termination of Salt Walls and Megaflaps: An Example from Gypsum Valley Diapir, Paradox Basin, Colorado: University of Barcelona.

Ferrill, D.A., 1991, Calcite Twin Widths and Intensities as Metamorphic Indicators in Natural Low-Temperature Deformation of Limestone: Journal of Structural Geology, v. 13/6, p. 667-75.

Friedman, I., and J.R. O'Neil, 1977, Compilation of Stable Isotope Fractionation Factors of Geochemical Interest: U. S. Geological Survey Professional Paper 440 KK, 12 p.

McArthur, J.M., R.J. Howarth, and G.A. Sheild, 2012, Chapter 7: Strontium Isotope Stratigraphy: in The Geologic Time Scale, 2012. F.M. Gredstein, J.G. Ogg, M.D. Schmotz, and G.M. Ogg (eds), Elsevier, vol. 1, p. 1144.

Rohrbaugh, Jr., M.B., W.M. Dunne, and M. Mauldon, 2002, Estimated Fracture Trace Intensity, Density, and Mean Length Using Circular Scan Lines and Windows: AAPG Bulletin, v. 86/12, p. 2089-2104.

Rybacki, E., B. Evans, C. Janssen, R. Wirth, and G. Dresen, 2013, Influence of Stress, Temperature, and Strain on Calcite Twins Constrained by Deformation Experiments: Tectonophysics, v. 601, pp. 20-36.

Sheppard, S.M.F., 1986, Characterizations and Isotopic Variations in Natural Waters: Reviews in Mineralogy and Geochemistry, v. 16, p. 165-183.

Trudgill, B.D., 2011, Evolution of Salt Structures in the Northern Paradox Basin: Controls on Evaporite Deposition, Salt Wall Growth and Supra-salt Stratigraphic Architecture: Basin Research, v. 23/2, p. 208-38.

Barrier vs. Conduit Behavior of Faults near Salt: Examples from the Gypsum Valley Salt Wall

Lillian R. Lueck and Mark P. Fischer

Department of Geology & Environmental Geosciences, Northern Illinois University, DeKalb, IL 60115

Motivation, Objective, and Approach

Rising salt bodies create unique deformation patterns and faulting associated with salt tectonics, creating a spatially complex network of high permeability pathways that can dramatically influence the movement of subsurface fluids in the vicinity of salt structures. Understanding the movement of fluids in the vicinity of these structures is critical for a variety of endeavors ranging from CO_2 sequestration, waste disposal, hydrocarbon exploration, and groundwater resources.

We aim to understand the hydrological significance of radial and counter-regional faults that often occur at the terminations of salt walls in the Paradox Basin.

We constrained paleohydrological behavior through (1) fieldwork, (2) GIS-based fracture network analysis, and (3) petrographic and isotopic analysis of fracture and host rock mineralization.

Geological Setting

We conducted our study at the southern end of the Gypsum Valley salt wall, in the Paradox Basin of southwestern Colorado (Figure 1). The Paradox Basin is a large asymmetric, intracratonic foreland basin with layered evaporites. Convergent tectonism along the western margin of North America, coupled with the collision of Gondwanaland to the south, created thick-skinned, basement-cored uplifts known as the Ancestral Rocky Mountains. The growing Uncompaghre Uplift shed fluvial sediments to the southwest during the Upper Pennsylvanian to Permian time (Figure 2). Differential loading of these sediments caused inflation of salt over preexisting normal faults and drove the growth of the linear salt walls in southwestern Colorado. (Figure 3; Trudgill, 2011; Escosa et al., 2018) In this study area the salt wall is cut by a down-to-the-northeast, counter-regional fault and two south-trending normal faults that bound a small graben.

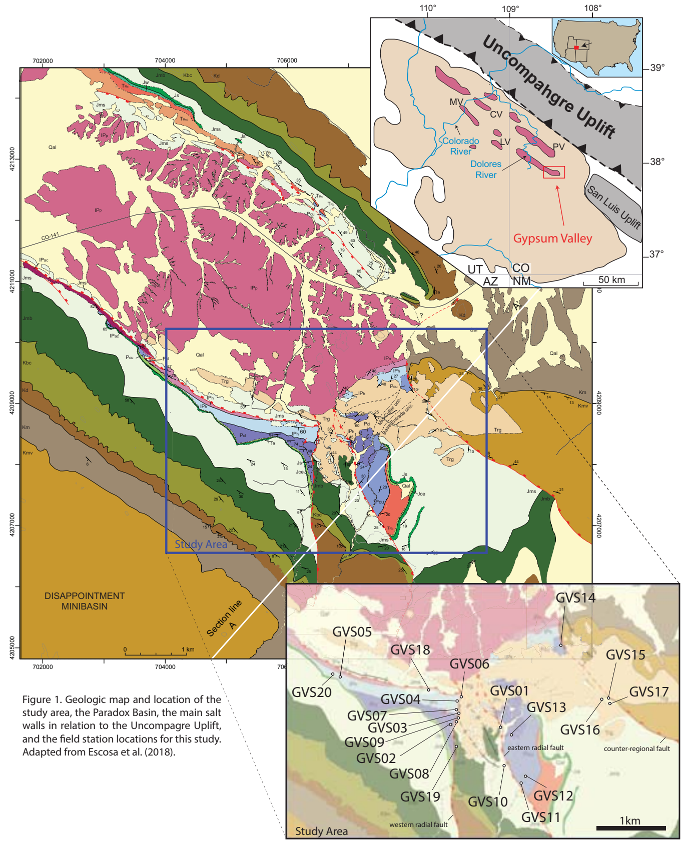

Figure 1. Geologic map and location of the study area, the Paradox Basin, the main salt walls in relation to the Uncompagre Uplift, and the field station locations for this study. Adapted from Escosa et al. (2018).

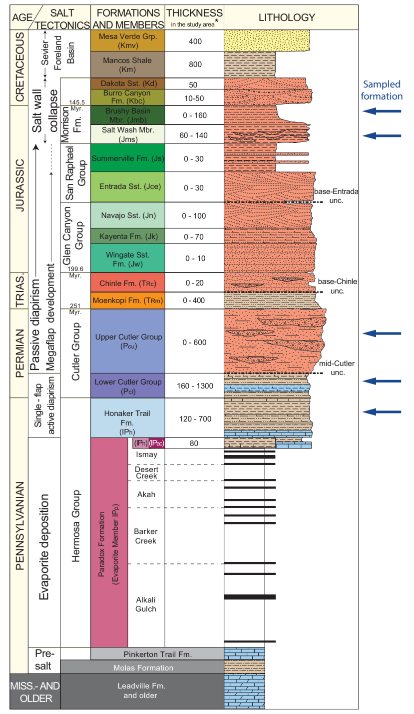

Figure 2. Stratigraphic column of the southern Paradox Basin. Blue arrows indicate units from which vein and/or host rock samples were collected. Adapted from Escosa et al. (2018).

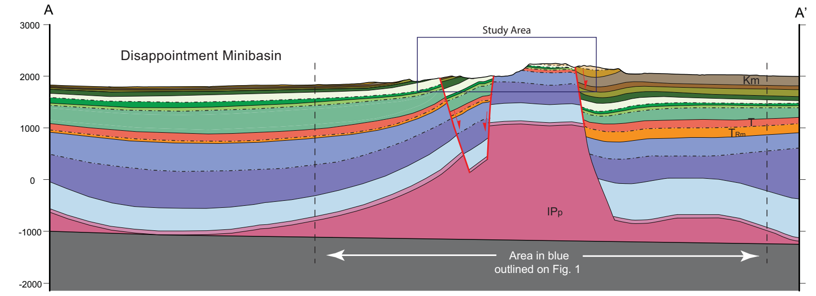

Figure 3. Cross section A-A' showing radial and counter-regional faults and the relative amount of throw along those faults. Adapted from Escosa et al. (2018). See Fig.1 for section location.

Fracture Network Analysis

We examined 20 outcrops on opposite sides of the faults and along the length of the faults as throw decreases to characterize the style (Figure 4), orientation (Figure 5), relative abundance (Figure 6), and timing (Figure 7) of fractures comprising the local network and to test for variability in those characteristics as a function of fault throw. Limited outcrop availability restricted our photogeological analysis of fracture abundance and focussed the majority of the stations along the western radial fault.

Fracture Style

Fractures are predominantly joints. Approximately 5-10% fractures are mineralized with calcite, and about 15% display minor faulting. Deformation bands are present but uncommon.

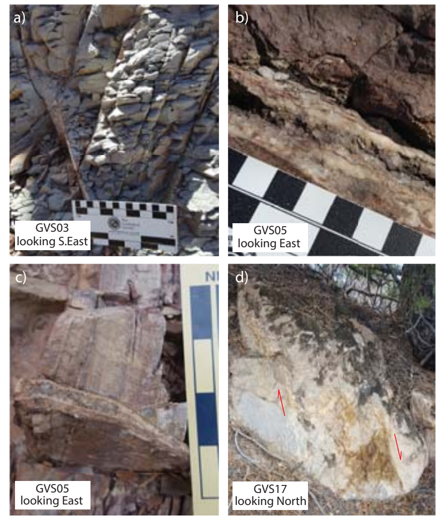

Figure 4. Photos from field stations in Gypsum Valley. a) Joints in outcrop at GVS03. b,c) Mineralized vein with crack-seal texture at GVS05. d) Riedel structure at GVS17, showing an east-side-down sense of motion.

Fracture Orientation

Orientations at each station of radial and concentric fractures around the nose of the plunging salt wall. Only three stations show clear timing relationships.

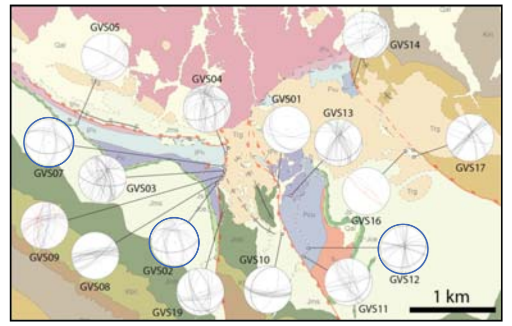

Figure 5. Fracture orientation at each station throughout the study area. Stereoplots outlined in blue mark the only stations with clear and consistent timing relationships amongst exposed fracture sets. Base map is adapted from Escosa et al. (2018).

Fracture Abundance

Fracture intensity (Rohrbaugh et al., 2002) was calculated by first digitizing photomosaics of bedding plane exposures of the fracture network at a given outcrop, and then dividing the summed length of all digitized fractures by the area of the outcrop. To test the variability of fracturing in relation to fault throw, six stations on opposite sides of the faults and with varying distance from the faults were photographed and the fractures were traced using ArcGIS.

Station Number	Structural Domain	Distance to Fault (m)	Area (m^2)	Fracture Intensity (m^{-1})	Stratigraphic Unit
GVS02	Western Fault - HW	5	10.35	12.15	Saltwash
GVS03	Western Fault - FW	10	11.47	3.02	Honaker Trail (?)
GVS04	Western Fault - FW	30	29.95	23.26	Honaker Trail
GVS09	Western Fault - HW	20	28.68	5.22	Saltwash
GVS11	Eastern Fault - FW	25	6.3	11.11	Upper Cutler
GVS12	Eastern Fault - FW	140	31.22	4.81	Upper Cutler

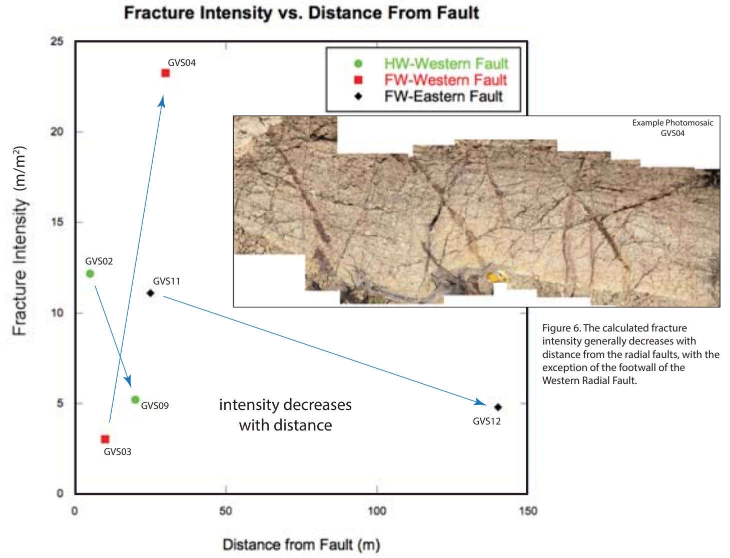

Figure 6. The calculated fracture intensity generally decreases with distance from the radial faults, with the exception of the footwall of the Western Radial Fault.

Fracture Timing

Timing determined by relationships of veins observed in the field.

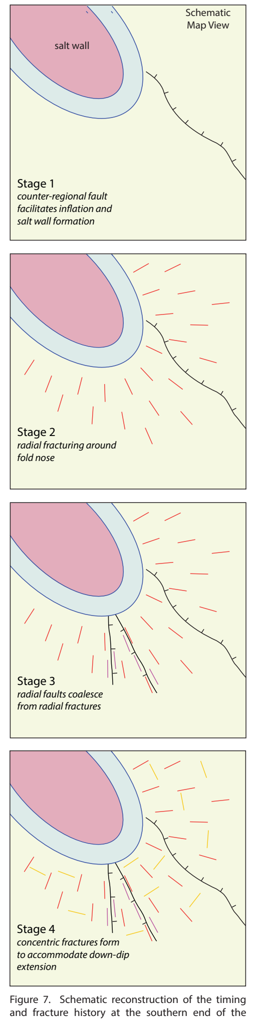

Figure 7. Schematic reconstruction of the timing and fracture history at the southern end of the Gypsum Valley salt wall.

Paleofluid System

We conducted stable isotope analyses of carbon and oxygen on select samples of vein and host rock calcite. In keeping with previous work (e.g., Bons et al., 2012), systematic stratigraphic or structural variations in the isotope values ($\delta^{18}O$ and $\delta^{13}C$) are intrepreted as a reflection of stratigraphical or structural control on the paleofluid system structure (e.g., fault compartmentalization).

Stable Isotope Analysis

Mineralized fractures are comprised of syntaxial calcite. Powdered samples from vein and host rocks (Figure 8) were analyzed using a ThermoFinnigan MAT253 Isotope Ratio Mass Spectrometer and the values ($\delta^{18}O$ and $\delta^{13}C$) plotted according to stratigraphic and structural positions (Figure 9). The data show two fluids, different from the host rock, moving through the veins in the system, implying this is an open system.

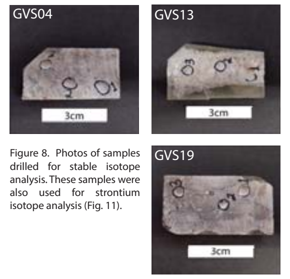

Figure 8. Photos of samples drilled for stable isotope analysis. These samples were also used for strontium isotope analysis (Fig. 11).

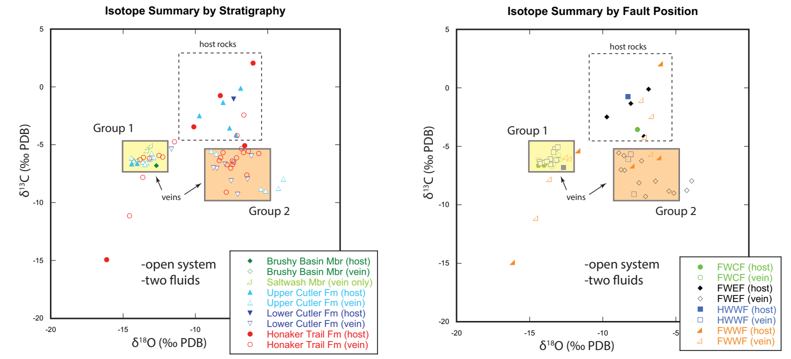

Figure 9. Carbon and oxygen stable isotopes plotted according to stratigraphy (left) and by structural position (right). Host material is shown as a solid symbol whereas veins are shown as an open symbol. Note the data tends to plot in two different groups that are different from the majority of the host rock. FWCF = Footwall of counter-regional fault, FWEF = Footwall of eastern radial fault, HWWF = hanging wall of western radial fault, FWWF = Footwall of western radial fault.

Paleofluid Constraints

The paleofluids that moved through the system have ambiguous origins. Fluid 1 could be organic, brine or meteoric water. Fluid 2 could be organic water (Figure 10; Sheppard, 1986). Paleofluids could be one fluid if the temperature difference between them is greater than 50°C or is very hot (>250°C). The temperature ranges for these fluids are poorly constrained and are based on twinning thickness. (Ferrill, 1991; Rybacki et al., 2013)

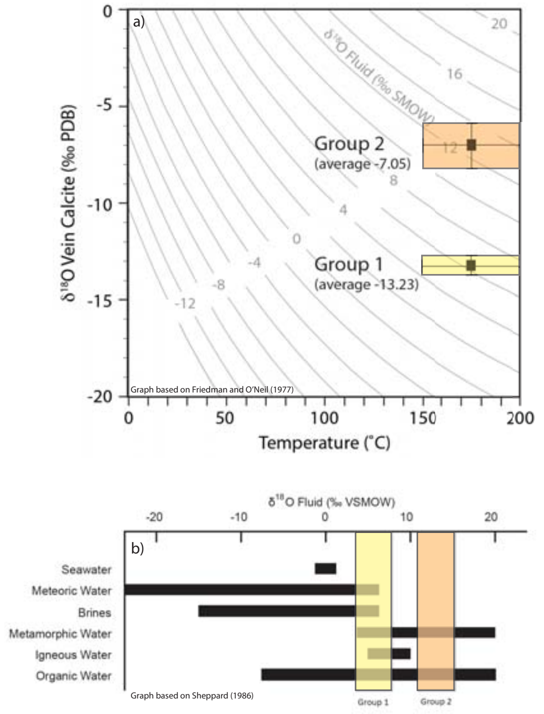

Figure 10. Graph (a) showing the stable isotope value of fluid based on the temperature of precipitation and the measured oxygen isotope value in calcite. The error bars in the y-direction represent the standard deviation of the data. Stable oxygen values for various types of fluids (b). The colored boxes represent the two groups of precipitated calcites.

Strontium Isotope Analysis

Powdered samples from seven stations on opposite sides of the faults were chosen for strontium isotope analysis at University of Texas - Austin. When the data are plotted against the LOWESS curve (Figure 11; McArthur, 2012), the data show the paleofluids moving through the system are different than marine fluids present at the time of deposition. This suggests an exotic fluid source.

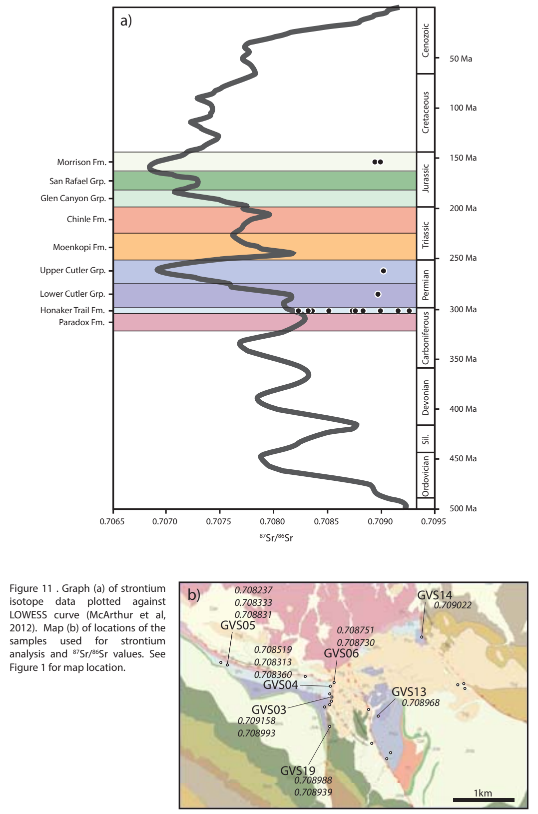

Figure 11 . Graph (a) of strontium isotope data plotted against LOWESS curve (McArthur et al, 2012). Map (b) of locations of the samples used for strontium analysis and $^{87}Sr/^{86}Sr$ values. See Figure 1 for map location.

Fault and Fracture Related Paleofluid System Summary

- Radial fractures formed first, later they coalesce to form radial faults.
- Concentric fractures formed last around the nose of the salt wall as suggested by field relations.
- Two exotic (i.e., externally derived) paleofluid types moved through the fracture network.
- The faults behaved as conduits for fluid movement as shown with increased fractures near faults, greater mineralization, and the presence of two fluid types (Figure 12).

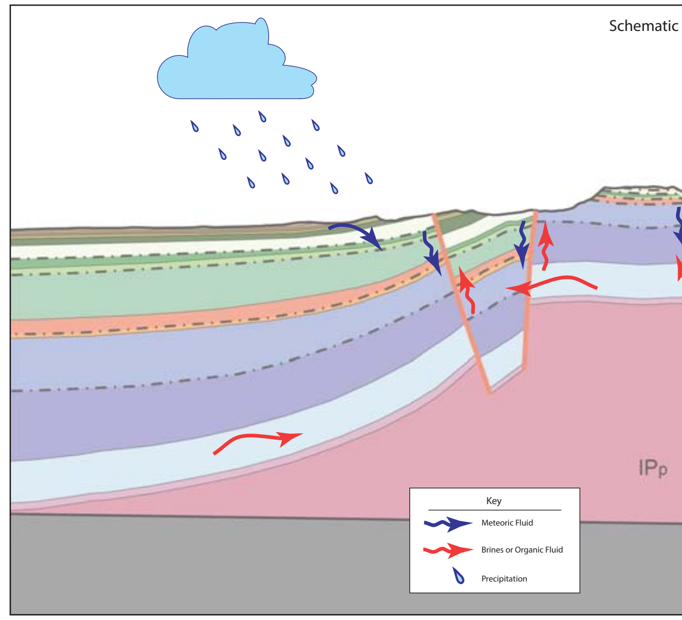

Figure 12. Schematic cross section showing patterns of paleofluid flow with mixing between basinal brines and meteoric water. Section adapted from Escosa et al (2018).

References

Bons, P. D., Elburg, M. A., Gomez-Rivas, E. (2012) A Review of the Formation of Tectonic Veins and Their Microstructures. Journal of Structural Geology, vol. 43, 2012, pp. 33-62.
Escosa, F. O., Rowan, M. G., Giles, K. A., Deatrick, K. T., Mast, A. M., Langford, R. P., Hearon IV, T. E., Roca, E. (2018) Lateral Termination of Salt Walls and Megaflaps: An Example from Gypsum Valley Diapir, Paradox Basin, Colorado. University of Barcelona
Ferrill, D. A. (1991) Calcite Twin Widths and Intensities as Metamorphic Indicators in Natural Low-Temperature Deformation of Limestone. Journal of Structural Geology, vol. 13, no. 6, pp. 667-75.
Friedman, I., and O'Neil, J. R. (1977) Compilation of Stable Isotope Fractionation Factors of Geochemical Interest. U. S. Geological Survey Professional Paper 440 KK, 12.p.
McArthur, J. M., Howarth, R. J., and Sheild, G. A. (2012) Chapter 7: Strontium Isotope Stratigraphy. In: The Geologic Time Scale, 2012. Gredstein, F. M., Ogg, J. G., Schmotz, M. D., and Ogg, G. M. Elsevier, vol. 1, p. 1144.
Rohrbaugh, M. B., Jr, Dunne, W. M., Mauldon, M. (2002) Estimated Fracture Trace Intensity, Density, and Mean Length Using Circular Scan Lines and Windows. AAPG Bulletin, vol. 86, no. 12, pp. 2089-104.
Rybacki, E., Evans, B., Janssen, C., Wirth, R., Dresen, G. (2013) Influence of Stress, Temperature, and Strain on Calcite Twins Constrained by Deformation Experiments. Tectonophysics, vol. 601, pp. 20-36.
Sheppard, S. M. F. (1986) Characterizations and Isotopic Variations in Natural Waters. Reviews in Mineralogy and Geochemistry, vol. 16, p. 165-183.
Trudgill, B. D. (2011) Evolution of Salt Structures in the Northern Paradox Basin: Controls on Evaporite Deposition, Salt Wall Growth and Supra-salt Stratigraphic Architecture. Basin Research, vol. 23, no. 2, pp. 208-38.

Acknowledgements

We would like to thank Seth Coursey for his assistance in the field, Nick Williams for running the isotope analysis, Kate Giles, Mark Rowan, and the present and past donors of the Salt-Sediment Interaction Research Consortium (S-SIRC).